medium. This could be a possible explanation for increase in calcium, magnesium, phosphate, etc. in the medium, after 7 days. This conclusion is also supported by an increase in the peak intensities of effluent X-ray spectra of days 9 and 11 (Figure 6).

Thus X-ray diffraction study, in addition to corroborating the results obtained by conventional methods, gives more specific information. It is a fast and more efficient method of monitoring the systematics of biomass–effluent interactions.

1. Tiwana, N. S., Nature and magnitude for water pollution in Punjab, Proceedings of Seminar on Status of Environmental Pollution, PAU, Ludhiana, 1985.
2. Subrahmanyam, P. V. R. and Mohan Rao, G. J., Treatment of dairy wastes by unmechanised methods. *Indian J. Environ. Health*, 1972, **14**, 236–245.
3. Pandit, B. R., Prasannakumar, P. G. and Kumar, M. R., Effect of dairy effluent on seed germination, seedling growth and pigment of *Pennisetum typhoides.* Barm. and *Sorghum bicolor* L., *Pollut. Res.*, 1996, **15**, 103–106.
4. Datar, M. T. and Kale, S. B., Performance of a dairy effluence treatment plant. *Indian J. Environ. Health*, 1997, **39**, 52–60.
5. Sharma, B. M., Aslam, M. and Gupta, H. O., Impact of industrial effluents on the aquatic system of the Doon valley. *J. Environ. Pollut.*, 2000, **7**, 59–65.
6. Chockalingam, S. and Balaji, A., Effect of dairy effluent on the rate of oxygen consumption and survival of the tadpole larva of *Bufo bufo*. *J. Environ. Biol.*, 1991, **12**, 377–379.
7. Amudha, P., Nagendran, R. and Mahalingam, S., Studies on the effects of dairy effluent on the behaviour of *Cyprinus carpio* (Cyprinidae). *J. Environ. Biol.*, 1997, **18**, 415–418.
8. Rai, R. K., Verma, S. and Goyle, M., Growth and biochemical profile of two cyanobacteria effected by carpet industry effluent. *Pollut. Res.*, 1999, **18**, 71–74.
9. Russell, P. J., The structure of genetic material. In *Genetics,* Addison Wesley, New York, 1998, pp. 303–304.
10. Davis, B. D., Dulbecco, R., Eisen, H. N. and Ginsberg, H. S., Antibody–antigen reactions. In *Microbiology*, Harper International Editions, Philadelphia, 1980, 3rd edn, pp. 292.
11. APHA, Standard methods for the examination of water and wastewater, American Public Health Association, AWWA and WPCF, Washington DC, 1985.
12. Mackinney, G., Absorption of light by chlorophyll solutions. *J. Biol. Chem.*, 1941, **140**, 315–322.
13. Kaushik, B. D., *Laboratory Methods for Blue Green Algae,* Associated Publishing Company, New Delhi, 1987, 1st edn, pp. 65–69.
14. Bredford, M. M., Rapid and sensitive method for the quantitation of microgram quantity of protein utilizing the principle of protein dye binding. *Ann. Biochem.*, 1976, **72**, 248–254.
15. Tandon, P., Further studies on the process of gall induction on *Zizyphus* and the factors involved. Ph. D. thesis, Jodhpur University, Jodhpur, India, 1976.
16. Manoharan, C. and Subramanian, G., Interaction between papermill effluent and the cyanobacterium *Oscillatoria pseudogerminata* var. *unigranulata. Pollut. Res.*, 1992, **11**, 73–84.
17. Manoharan, C. and Subramanian, G., Feasibility studies on using cyanobacteria in ossein effluent treatment. *Indian J. Environ. Health*, 1993, **35**, 88–96.
18. Dash, A. K. and Mishra, P. C., Role of blue green alga *Westiellopsis prolifica* in reducing pollution load from paper mill wastewater. *Indian J. Environ. Protect.*, 1999, **19**, 1–5.
19. Mittal, S. and Sengar, R. M. S., Toxic effect of sulphate and its uptake in algae. *Natl. Acad. Sci. Lett.*, 1989, **12**, 17–19.
20. Tam, N. F. Y. and Wong, Y. S., The comparison of growth and nutrient removal efficiency of *Chlorella pyrenoidosa* in settled and activated sewages. *Environ. Pollut.*, 1990, **65**, 93–108.
21. Manoharan, C. and Subramanian, G., Sewage–cyanobacterial interaction – a case study. *Indian J. Environ. Protect.*, 1992, **12**, 251–258.
22. Fallowfield, H. D. and Barret, M. K., The treatment of wastes by algal culture. *Agric. Wastes*, 1985, **12**, 111–136.
23. Uma, L. and Subramanian, G., Effective use of cyanobacteria in effluent treatment. Proceedings of the National Symposium on Cyanobacterial Nitrogen Fixation, IARI, New Delhi, 1990, pp. 437–444.
24. Meusel, I., Barthlott, W., Kutzke, H. and Barbier, B., Crystallographic studies of plant waxes. *Powder Diffr.*, 2000, **15**, 123–129.
25. William, F. M. (ed.), Powder diffraction file, organic and organometallic phases search manual, ICDD 1998, Card numbers a: 37–1943; b: 36–1744; c: 27–1665; d: 38–1212; e: 1–567.

ACKNOWLEDGEMENTS. This work has been partly supported by UGC DRS COSIST programme to the Department of Physics, M. L. Sukhadia University Udaipur, and also by the DST (Rajasthan).

Received 20 January 2003; revised accepted 18 September 2003

Structural characteristics of marine atmospheric boundary layer and its associated dynamics over the Central Arabian Sea during INDOEX, IFP-99 campaign

D. Bala Subrahamanyam* and Radhika Ramachandran†

Space Physics Laboratory, Vikram Sarabhai Space Centre, Thiruvananthapuram 695 022, India
*Present address: Indian National Centre for Ocean Information Services, Department of Ocean Development, Hyderabad 500 033, India

The Indian component of the Intensive Field Phase of Indian Ocean Experiment conducted onboard Oceanic Research Vessel *Sagar Kanya* during its SK-141 cruise provided valuable meteorological data over the data-sparse region of tropical Indian Ocean and Central Arabian Sea (CAS). The upper air meteorological data obtained from balloon-borne GLASS sonde launches during the campaign are analysed for studying the thermodynamic structure of the Marine Atmospheric Boundary Layer over the CAS. Analysis of profiles of the thermodynamic variables revealed a double mixed layer structure over the region of CAS. We have made an attempt here to provide a possible explanation of the double mixed layer.

THE Indian Ocean Experiment (INDOEX), a major international and multi-disciplinary field experiment, had several objectives focused towards the studies of aerosols, radiation and transport of pollutants over the western tropical Indian Ocean region[1,2]. The Indian component of the

†For correspondence. (e-mail: radhika@md3.vsnl.net.in)

INDOEX observations was conducted onboard Oceanic Research Vessel (ORV) *Sagar Kanya* in four consecutive years 1996–1999, with different cruise paths covering a broad oceanic region of the western tropical Indian Ocean during the Northern Hemispheric Winter Monsoon period[1]. The present study is focused on the meteorological data collected over the Central Arabian Sea (CAS) during the Intensive Field Phase of INDOEX (INDOEX, IFP-99). Figure 1 shows the cruise track of INDOEX, IFP-99 campaign. The approximate position of the ship on various Julian days is marked on the cruise track. The altitude profiles of thermodynamic parameters along track-DEFA show a double mixed layer structure with shallow mixed layer heights. The main objective of this paper is to explain the double mixed layer structure observed over the CAS region. To understand the plausible causes for the formation of such an atypical structure and its associated dynamics, we present the analysis of the vertical structure of the Marine Atmospheric Boundary layer (MABL) and the air–sea interaction parameters as a function of Julian day over the CAS, where such a structure is seen.

During the IFP-99 campaign, MABL experiments were carried out by mounting various meteorological sensors on a 7-m long retractable boom close to the ship bow at an altitude of about 10-m above the sea surface. Further details on the data acquisition system, various sensors used in the study and their accuracies are described elsewhere[3–8]. Surface layer meteorological data collected from these sensors are used for the estimation of air–sea interaction parameters using the revised bulk algorithm[3,7] based on the bulk algorithm suggested by Smith[9]. Apart from the surface measurements taken onboard ship, balloon-borne GLASS (GPS Loran Atmospheric Sounding System) sondes were launched from the ship to measure the pressure, temperature, humidity and wind[8]. GLASS sonde launches provide time series of pressure, temperature, humidity and wind in the vertical up to an altitude of 20 to 25 km at the rate of approximately 1 Hz. After eliminating obviously bad data points, all the profiles are interpolated at an interval of 50 m each in the vertical and we believe that such an interpolation will preserve the vertical thermodynamic profiles of the individual sounding to a good extent. Individual values of observed meteorological parameters from the raw data that differed by more than two standard deviations from the mean were considered as spikes and therefore eliminated from the respective data. Since our aim is to study the characteristic features of the MABL, we have confined our analysis of all the profiles to an altitude of 5000 m. After interpolating the raw data into 50-m level each in the vertical, the observed values of temperature (T), humidity (RH) and pressure (P) are used for the computation of thermodynamic parameters such as specific humidity (q), potential temperature (θ), virtual potential temperature (θ_V), equivalent potential temperature (θ_E), saturation equivalent potential temperature (θ_{ES}) and parcel saturation pressure difference (P_{SPD}, defined as the difference between ambient pressure and saturation level pressure)[8,10–14].

The profiles of meteorological and thermodynamic parameters (wind speed (WS), relative humidity (RH), wind direction (WD), zonal and meridional wind components (u and v), virtual potential temperature (θ_V), specific humidity (q), equivalent potential temperature (θ_E), saturation equivalent potential temperature (θ_{ES}) and parcel saturation pressure difference (P_{SPD})) over the CAS (14.59°N; 61.15°E) observed on 2 March 1999 (1228 GMT) are shown in Figure 2. Analysis of altitude profiles of θ_V and q is found in the literature for the identification of the top of

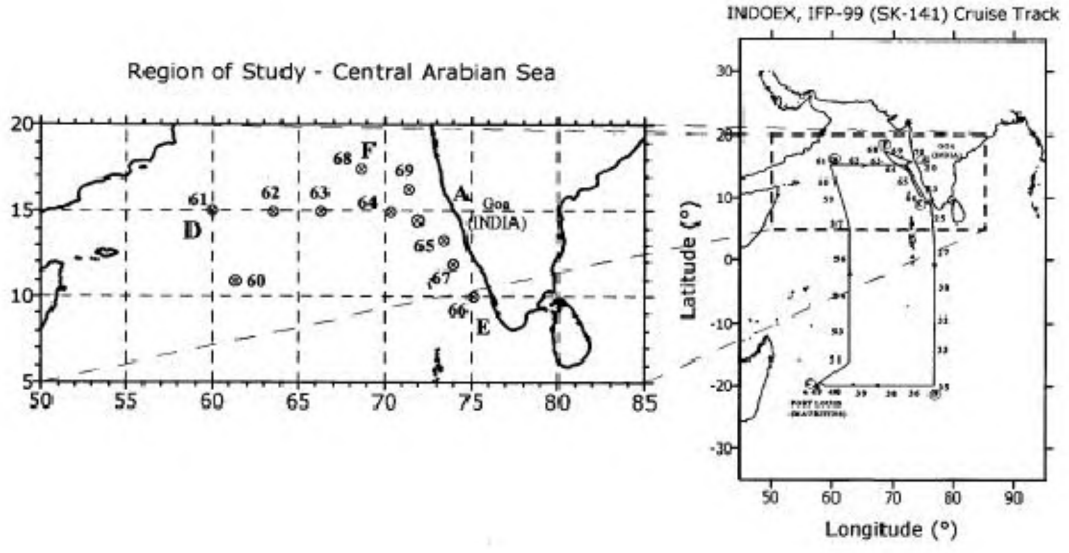

Figure 1. Cruise track of INDOEX, IFP-99 conducted onboard ORV *Sagar Kanya*. (Julian day numbers are marked on the cruise track to represent the approximate position of the ship during that day.)

convective mixed layer[8,15–23]. In general, the tendency of θ_V and q profiles is to be constant within the mixed layer due to the turbulent-mixing mechanism. Above the mixed layer, θ_V and q profiles show a sharp gradient. Therefore, the convective mixed layer heights, in general, are considered at the height, where the first significant gradient in profiles of θ_V and q is seen[23]. In the present analysis, we have identified the depth of the mixed layer by noting the height at which this significant inversion in θ_V and q profiles is evident. Also, within the mixed layer, the gradients of θ_V should not exceed 2 K/km (ref. 22). Profiles of thermodynamic parameters show the double mixed layer structure (Figure 2). Profiles of WS, RH, WD, u and v show a large gradient in the magnitudes at a particular altitude of about 500 m. Wind speed is seen to increase in the lower layers (typically < 500 m) with height; however, such an increase is not seen above 500 m (Figure 2 *a*). Above 500 m, a sudden drop in wind speed is apparent. As we go higher in altitudes, wind speed does not show any large variation, but remain constant (~ 6 ms^{-1}) up to an altitude of about 4500 m. Profiles of RH show higher values in the lower region (< 500 m). At an altitude of about 500 m, a sudden drop in RH (from 90% to 20%) is observed. Profiles of WD show two distinct regions, one with easterly winds (WD = ~ 90°, below 3000 m) and the other with westerly winds (WD = ~ 270°, between 3000 m and 4500 m). Such a wind pattern suggests the existence of an anticyclone over the CAS. Profiles of u and v wind component also confirm such a circulation (Figure 2 *d*, *e*). Figure 2 *f*–*j* shows the profiles of thermodynamic parameters (θ_V, q, θ_E, θ_{ES} and P_{SPD}). From these profiles, two distinct mixed layers are seen (one from surface to an altitude of about 400 m and the other from 900 m to 2700 m). In these layers, θ_V, q and θ_E remain constant, whereas θ_{ES} decreases with altitude and P_{SPD} increases with altitude.

For a complete understanding of the underlying physics of the double mixed layer structure, we show in Figure 3 *a* typical daytime convective boundary layer profiles of θ_V and q corresponding to 1400 LT along cruise track-DEFA. Profiles of q are biased by 300 g kg^{-1} to enable simultaneous display of q along with θ_V profiles. The top of the mixed layer, lifting condensation level (LCL) and trade wind inversion, inferred from these profiles are shown in Figure 3 *b*. In this variation of trade wind inversion, mixed layer height and LCL are shown against the respective Julian days. Also shown in the figure is the calendar date corresponding to the Julian day for an easier interpretation. The trade wind inversion, which acts as an interface between the mixed layer and the free atmosphere, is marked by a maximum of θ_{ES} and a corresponding minimum in P_{SPD} and θ_E (ref. 24). Profiles of θ_V and q along cruise track-DEFA show interesting features over the CAS, with double mixed layer structure prevailing over the western sector of the track. Because of turbulent mixing, the altitude profiles of θ_V and q show almost constant values in the mixed layer extending from the surface to the base of the stable layer, where there is a sharp gradient in the

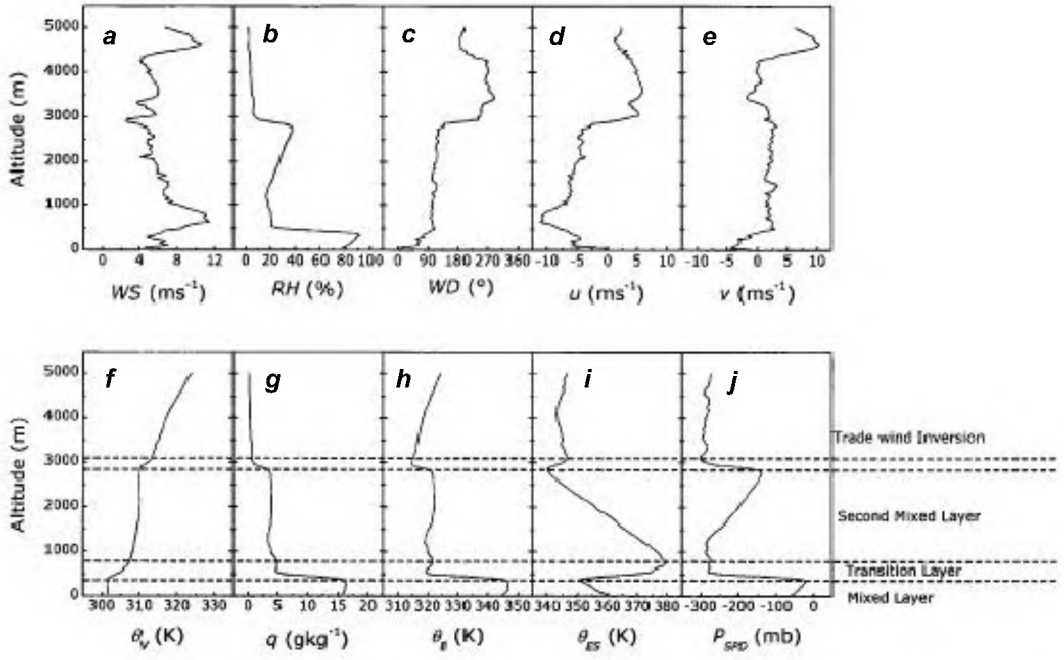

Figure 2. Profiles of (***a***) wind speed (WS), (***b***) relative humidity (RH), (***c***) wind direction (WD), (***d***) zonal wind component (U), (***e***) meridional wind component V, (***f***) virtual potential temperature (θ_V), (***g***) specific humidity (q), (***h***) equivalent potential temperature (θ_E), (***i***) saturation equivalent potential temperature (θ_{ES}) and (***j***) parcel saturation pressure difference (P_{SPD}) on 2 March 1999 (1228 GMT). (Location of GLASS sonde launch: 14.59°N; 61.15°E.)

magnitudes of θ_V and q (Figure 3 *a*). Above this inversion layer, the magnitudes of θ_V and q remain almost constant up to an altitude of about 3 km. This thick layer with constant θ_V and q values is designated as the second mixed layer. Profiles of q observed along track-DEFA show that the magnitudes of q in the second mixed layer is considerably lower than those of the first mixed layer—extending from the surface to the base of stable layer (approximately at about 600 m). Hence, it can be inferred from the specific humidity profiles that the second mixed layer consists of relatively dry air mass when compared to the first mixed layer. It also confirms that the first and second mixed layers have different air masses and that they are not linked directly. Such a double mixed layer structure is quite apparent in all the profiles of θ_V and q observed between Julian days 60 and 65 (1–6 March 1999; Figure 3 *a*). However, the structure is seen to gradually disappear during the rest of the days (7–11 March 1999) while the ship was moving towards the western coastline of the Indian subcontinent. The mixed layer height variation along track-DEFA lies within a range of 300 m to 800 m with an average value of about 560 m (Figure 3 *b*). The altitude of LCL, often considered as the height of the cloud base, is also shown in Figure 3 *b*. The LCL altitudes along track-DEFA over the CAS region varied between 250 m and 1050 m with an average value of about 680 m. It is apparent from Figure 3 *b* that in most of the cases, the LCL is higher than that of the height of the mixed layer. On certain occasions, the mixed layer heights are greater than those of the LCL, thereby implying saturation in the upper portion of the mixed layer. If LCL is more than the height of the mixed layer, then there is a possibility of the decoupling of the mixed layer with the clouds. The altitude of trade wind inversion over the CAS region along the cruise track varied within a range of 2500–3800 m.

On the basis of the estimated thermodynamic parameters from GLASS sonde launches, we now attempt a conserved variable analysis (CVA) of a subset of the estimated parameters θ_E and q, which is useful for diagnostic studies on boundary layer processes and the thermodynamic structure of MABL. Figure 4 *b* shows an idealized CVA plot between θ_E and q that depicts the mixing line and effect of precipitation and radiative cooling on air parcel saturation point. The movement of an air-parcel and its associated thermodynamic processes can be studied from the CVA. During a radiative process the magnitudes of q will not change, but radiative cooling moves points to lower θ_E at constant q. The CBL mixing line shows intense mixing of the lower atmospheric constituents

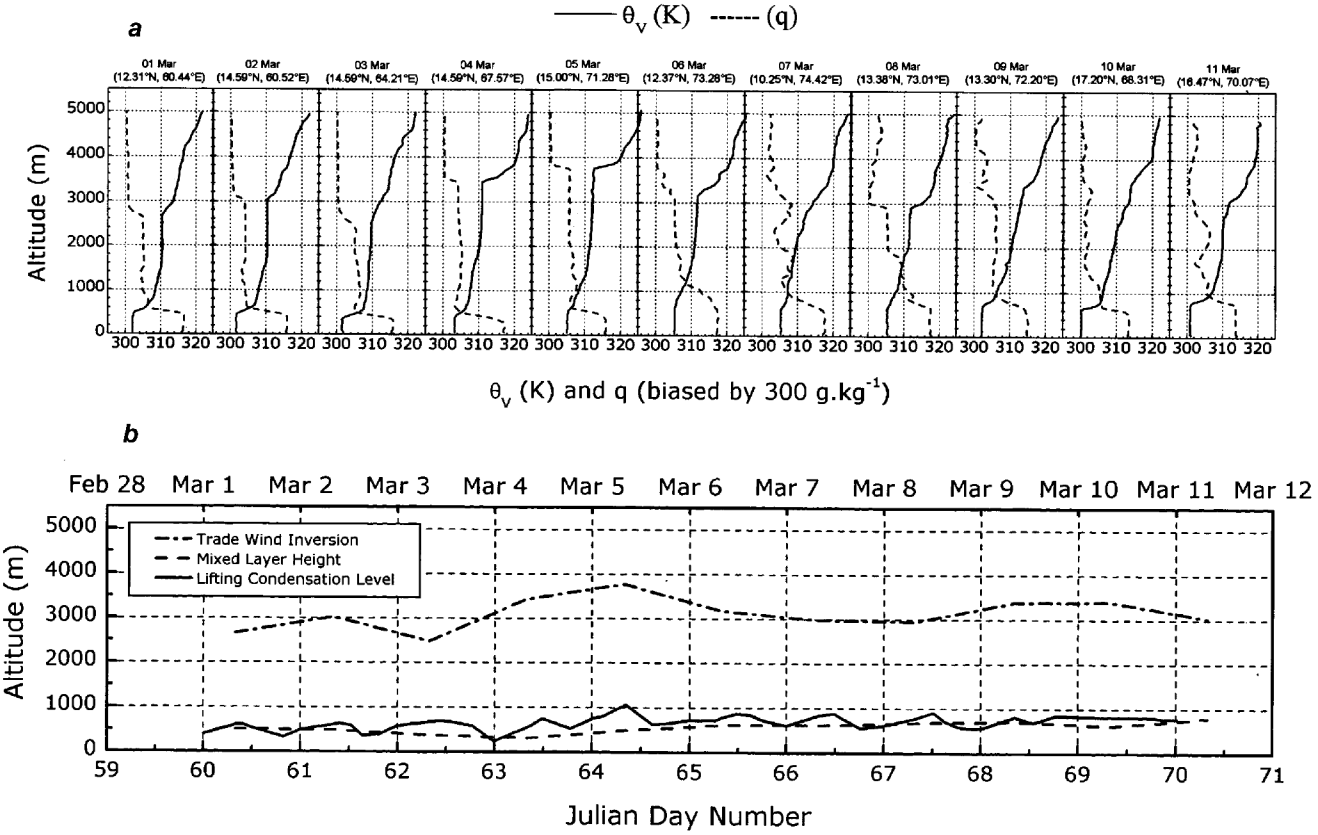

Figure 3. ***a***, Daytime convective boundary layer profiles of θ_V (K) and q (biased by 300 gkg^{-1}) corresponding to 1400 LT along cruise track-DEFA over the CAS region during 1–11 March 1999. ***b***, Mixed layer heights, lifting condensation level and trade wind inversion variation corresponding to the above profiles.

within the mixed layer. During the process of precipitation within the MABL, the air-parcel is moved from the subcloud layer to the lower q, at constant θ_E. Figure 4 *a* shows the CVA plots between θ_E and q for the typical daytime convective boundary layer profiles corresponding to 1400 LT along the cruise track-DEFA over the CAS region. In the figure, q-axis is reversed so that a sounding plotted superficially resembles a more familiar ($\theta_E - P$) plot. Figure 4 *a* shows CVA plots between θ_E and q for 11 consecutive Julian days (from Julian day 60 to 70, i.e. 1–11 March 1999). The CVA plots during 1–6 March 1999 show a peculiar double mixing line structure with a small q reversal at lower altitudes (about 550 m), almost similar to that at higher altitudes of trade wind inversion (about 3000 m). However, such a double mixing line structure is not prominent in the rest of the profiles during 7–11 March 1999.

The wind speed and wind direction profiles along the cruise track-DEFA over CAS region are shown in Figure 5. Wind speed profiles for 7 March and 11 March are not available owing to instrumentation problem, so also the wind direction profile for 11 March. Figure 5 *a* and *b* suggests an anti-cyclonic circulation over the CAS region with the existence of two different wind direction regimes below the trade wind inversion. On closer observation, the wind direction structure over the CAS region revealed the existence of westerly (or north-westerly) winds at lower altitudes (< 500 m) and easterly (or south-easterly) winds prevailing at higher altitudes (between 500 m and 3000 m). In almost all the profiles, a sudden change in the wind direction coincides with large wind shears. Sudden changes in the wind direction at different altitudes observed in the profiles confirm that the air mass existing at different altitudes is a result of horizontal advection of different boundary layers. The mixed layer extending from the sea surface to an altitude where the sharp gradients in thermodynamic parameters are imminent is driven by surface layer fluxes. Due to strong turbulent mixing, the profiles of the thermodynamic parameters such as θ_V and q tend to be constant within the mixed layer. The second mixed layer (between ~ 550 m and ~ 3000 m) with constant θ_V and q, can be attributed to processes that are responsible for changes in the saturation parameters. Perhaps the processes of radiative warming/cooling or evaporation of descending air parcel within the second mixed layer can be one of the causes of the existence of such double mixing line structure.

Figure 6 shows the behaviour of air–sea interaction parameters along track-DEFA. In this figure is shown the spatio-temporal variation of (a) sea surface temperature (SST) and air temperature (AT), (b) relative humidity (RH) and pressure (PRES), (c) wind speed (WS) and wind direction (WD) and (d) sensible heat flux (SHF) and latent heat flux (LHF). As described earlier, the double mixed layer structure observed over the CAS is prominent during Julian days 60–65, and as the ship approaches the western

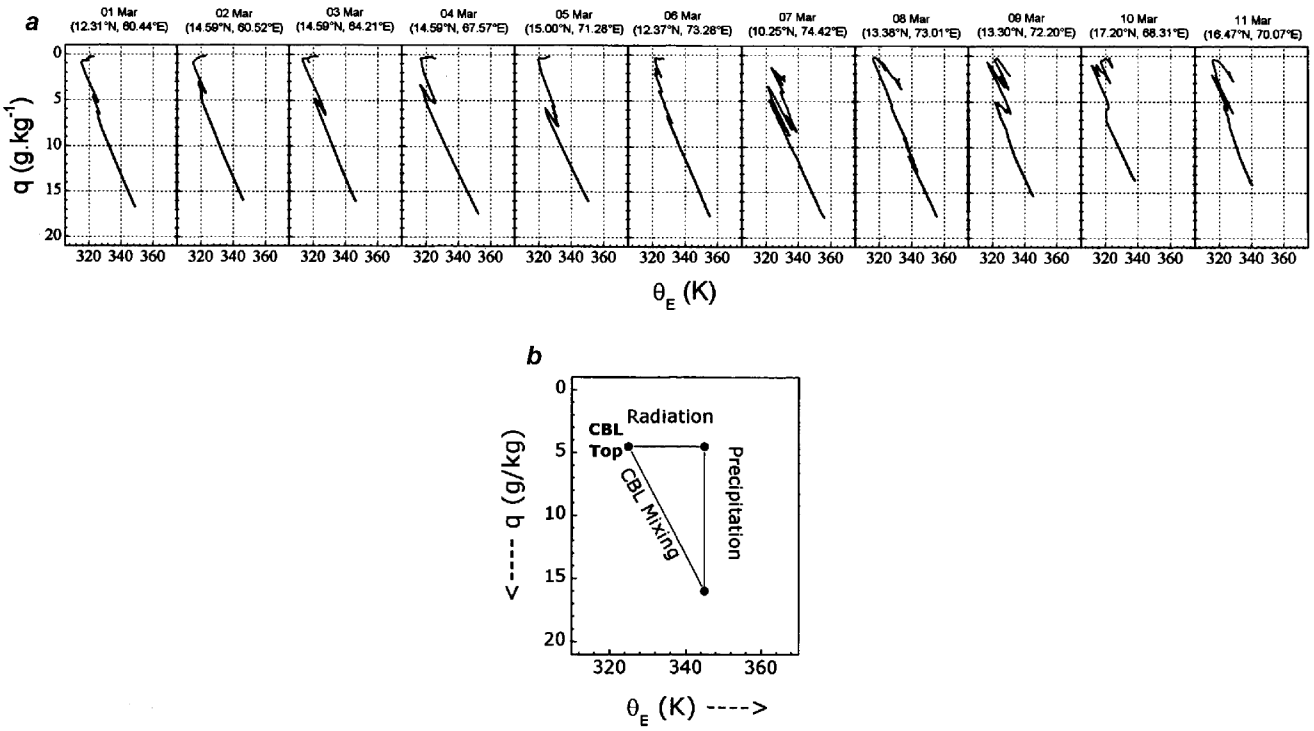

Figure 4. *a*, Conserved variable analysis plots between θ_E and q for the typical daytime convective boundary layer profiles corresponding to 1400 LT along the cruise track-DEFA over the CAS. *b*, Schematic representation of CVA showing various thermodynamic processes within the MABL, such as radiative cooling, CBL mixing, precipitation and the respective behaviour of θ_E and q.

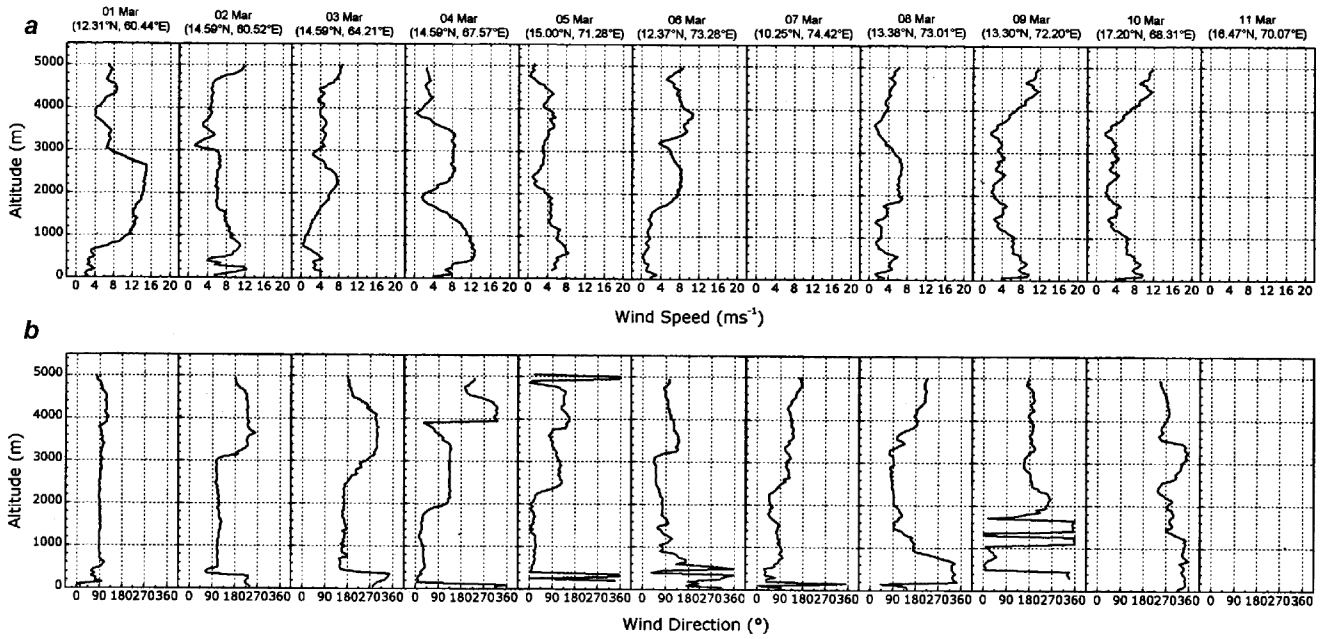

Figure 5. Wind speed (*a*) and wind direction (*b*) profiles corresponding to 1400 LT along cruise track-DEFA over the CAS region during 1–11 March 1999.

coast (after Julian day 65), such a structure disappears. Now we shall analyse the spatio-temporal variation of the above parameters in the vicinity of two conditions, when the double mixed layer structure is prominent and when it disappears. The magnitudes of SST exceed AT over most of the track; higher temperatures are seen towards the Indian western coast (Figure 6 *a*). On comparison with the existence of the double mixed layer structure, we notice that as SST and AT start increasing near the western coast (after Julian day 64–65), the double mixed layer structure disappears. The spatio-temporal variation of RH and PRES is shown in Figure 6 *b*, where it is evident that the RH values varied within a range of 70–90%. Except for the first two Julian days (i.e. 60–62), the RH values were always less than 80% for days 62–70, a small diurnal component is evident in the RH variations along the track. A variation between 1005 and 1015 mb is evident from the figure. During Julian days 60–66, a decreasing trend in surface pressure is observed. Though not very well identified, a diurnal component in surface pressure can be seen from the pressure variations along this part of the cruise track. It is to be noted that the western sector of the cruise track (near point 'D' in Figure 1) shows large surface pressure values compared to the eastern sector close to the Indian subcontinent. Figure 6 *c* shows the spatio-temporal variation of surface wind speed along the cruise track over the CAS region. From this figure, it can be seen that, except for the Julian day 67, the surface winds were, in general, below 8 ms^{-1}. In particular, during Julian days 64–66, winds were below 4 ms^{-1}. Disappearance of the double mixed layer structure (Julian day 65 onwards) coincides with a gradual increase in

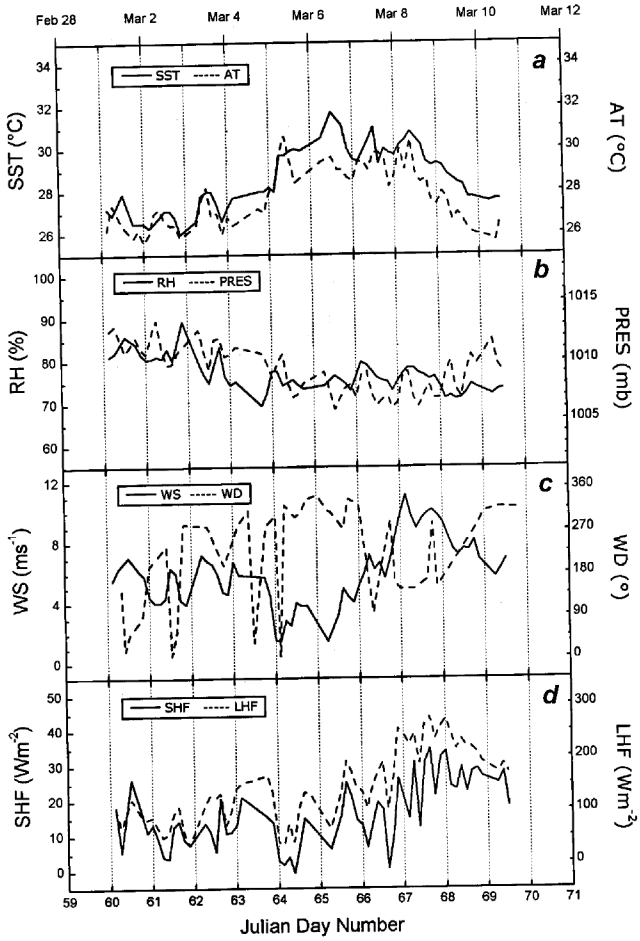

Figure 6. Spatio-temporal variation of: *a*, sea surface temperature (SST) and air temperature (AT); *b*, relative humidity and pressure; *c*, wind speed (WS) and wind direction; sensible heat flux and latent heat flux.

wind speed, as the ship came in the proximity of the western coast. Figure 6 *c* also shows the spatio-temporal variation of WD. An irregular behaviour in the variations in WD values is evident from the figure. Still, for most of the time, westerly winds (WD in the range 180°–360°) are seen. Spatio-temporal variations of air–sea interface fluxes of heat and moisture are shown in Figures 6 *d*. Estimates of SHF magnitudes varied within a range of about 0 Wm^{-2} to 35 Wm^{-2}, with an average of about 17 Wm^{-2} (Figure 6 *d*). LHF estimates over the CAS region show a variation within a range between 30 Wm^{-2} and 275 Wm^{-2}, with an average value of about 145 Wm^{-2}. As seen in the variation of SST, AT and WS, the estimates of air–sea interface fluxes also show an increasing trend after Julian day 65. Probably the disappearance of the double mixed layer structure near the western coast (during Julian day 66–70) has a direct bearing on the increased air–sea interaction parameters after Julian day 65.

Similar studies conducted over the Atlantic Ocean during the Barbados Oceanographic and Meteorological Experiment (BOMEX) also revealed multiple mixed layer structure[24]. Betts and Albrecht[24] have explained this to be the result of precipitation–evaporation processes. Similar observation of the double mixed layer structure has also been reported over the CAS during INDOEX, IFP-99 conducted onboard the research vessel *Ronald H. Brown*[23] and Bay of Bengal during the Bay Of Bengal Monsoon Experiment (BOBMEX)[25], where the investigators have speculated the differential advection of boundary layers to be a possibility[23,25]. We are not able to explain the mechanism responsible for the formation of a double mixed layer; however, we observe that this double mixed layer structure is dissipated as the coastline is approached. Perhaps the mesoscale circulations that develop along coastlines, for example, the internal boundary layers, could be the reason.

With the existing database, it was not possible to provide a distinct snapshot of the double mixed layer structure completely, as the data collected onboard ORV *Sagar Kanya* provided a spatio-temporal variation when the ship was in continuous movement. In future, one has to make a meticulous plan of the cruise tracks exclusively to study the double mixed layer formation and its dynamics. Only then will a coherent picture emerge of this interesting feature that has been observed over the CAS. Further studies will be required to understand the mechanism for the formation of such a double mixed layer.

1. Mitra, A. P., *Curr. Sci.* (*Suppl.*), 2001, **80**, 3–6.
2. Ramanathan, V. *et al.*, *J. Geophys. Res.*, 2001, **106**, 28371–28398.
3. Subrahamanyam, D. B. and Radhika, R., *J. Atmos. Sol. Terr. Phys.*, 2002a, **64/3**, 291–305.
4. Subrahamanyam, D. B., Radhika, R., Sen Gupta, K., Praveena, K., Kunhikrishnan, P. K. and Sudha, R., Marine Atmospheric Boundary Layer (MABL) Studies over the Indian Ocean during INDOEX, IFP-99, SPL Scientific Report, 2002, (Also available at: http://www.geocities.com/subbu_dbs/INDOEX/report_ifp.pdf).
5. Subrahamanyam, D. B., Sen Gupta, K., Sudha, R. and Praveena, K., *Curr. Sci.* (*Suppl.*), 2001, **80**, 85–88.
6. Subrahamanyam, D. B. *et al.*, Proceedings of the Symposium TROPMET 2000 on Ocean and Atmosphere, 2001, pp. 410–414.
7. Subrahamanyam, D. B. and Radhika, R., *Ann. Geophys.*, 2003, (in press).
8. Subrahamanyam, D. B., Radhika, R., Sen Gupta, K. and Mandal, T. K., *Boundary-Layer Meteorol.*, 2003, **107**, 683–695.
9. Smith, S. D., *J. Geophys. Res.*, 1988, **93**, 15467–15472.
10. Betts, A. K., *J. Atmos. Sci.*, 1982, **39**, 1484–1505.
11. Bolton, D., *Mon. Weather Rev.*, 1980, **108**, 1046–1053.
12. Plate, E. J., *Engineering Meteorology*, Elsevier, Amsterdam, 1982, pp. 740.
13. Schubert, W. H. *et al.*, Colorado State University Report, Atmospheric Science Paper No. 512, 1992, p. 96.
14. Stull, R. B., *An Introduction to Boundary Layer Meteorology*, Kluwer, Dordrecht, 1988, pp. 666.
15. Garratt, J. R., *The Atmospheric Boundary Layer*, Cambridge University Press, 1992, pp. 316.
16. Holt, T. and Raman, S., *Boundary-Layer Meteorol.*, 1985, **33**, 259–282.
17. Holt, T. and Raman, S., *Mon. Weather Rev.*, 1986, **114**, 2176–2190.
18. Holt, T. and Raman, S., *MAUSAM*, 1987, **38**, 171–176.
19. Lambert, D. and Durand, P., *Q. J. R. Meteorol. Soc.*, 1999, **125**, 495–512.
20. Lambert, D., Durand, P., Thoumieux, F., Benech, B. and Druilhet, A., *Q. J. R. Meteorol. Soc.*, 1999, **125**, 513–528.
21. Manghanani, V. *et al.*, *Boundary-Layer Meteorol.*, 2000, **97**, 411–430.
22. Parasnis, S. S. and Morwal, S. B., *Boundary-Layer Meteorol.*, 1993, **63**, 365–380.
23. Satyanarayana, A. N. V. *et al.*, *Curr. Sci.* (*Suppl.*), 2001, **80**, 39–45.
24. Betts, A. K. and Albrecht, B. A., *J. Atmos. Sci.*, 1987, **44**, 83–99.
25. Sam, N. V., Mohanty, U. C. and Satyanarayana, A. N. V., *Proc. Indian Acad. Sci.* (*Earth Planet. Sci.*), 2000, **109**, 305–314.

ACKNOWLEDGEMENTS. We are grateful to Dr A. P. Mitra, Chairman, National Steering Committee, Shri G. Viswanathan, Program Director, INDOEX-India Program, Dr N. Bahulayan, Chief Scientist onboard ORV *Sagar Kanya* and all the members of the Indian component of INDOEX program for their strenuous efforts for making the Indian component of the campaign a great success. We thank the efforts put forward by Dr K. Sen Gupta, former head of BLP branch of SPL, VSSC in INDOEX. The GLASS Sonde profile data was made available by Dr Tuhin K. Mandal, NPL, New Delhi, and is acknowledged. Subrahamanyam thanks ISRO for providing a Research Fellowship. We also thank an anonymous reviewer, whose comments greatly improved the contents of the paper.

Received 10 October 2002; revised accepted 16 July 2003